

The uncoupled chloride conductance of a bacterial glutamate transporter homolog

Rena M Ryan & Joseph A Mindell

Glutamate transporters (EAATs) are pivotal in mammalian synaptic transmission, tightly regulating synaptic levels of this excitatory neurotransmitter. In addition to coupled glutamate transport, the EAATs also show an uncoupled Cl⁻ conductance, whose physiological importance has recently been demonstrated. Little is yet known about the molecular mechanism of chloride permeation. Here we show that Glt_{ph}, a bacterial EAAT homolog whose structure has been determined, displays an uncoupled Cl⁻ conductance that can determine the rate of substrate uptake. A mutation analogous to one known to specifically affect Cl⁻ movement in EAAT1 has similar effects on Glt_{ph}, suggesting that this protein is an excellent structural model for understanding Cl⁻ permeation through the EAATs. We also observed an uncoupled Cl⁻ conductance in another bacterial EAAT homolog but not in a homolog of the Na⁺/Cl⁻-coupled neurotransmitter transporters.

Glutamate is the predominant excitatory neurotransmitter in the mammalian central nervous system, activating a wide range of ionotropic and metabotropic receptors that shape synaptic responses. The extracellular glutamate concentration is controlled by a family of EAATs, which take up the neurotransmitter into glia and neurons. Failure or downregulation of EAAT function leads to elevations in extracellular glutamate concentrations, which, if prolonged, result in excitotoxicity and neuronal cell death. Defective function and regulation of EAATs has been implicated in multiple human diseases, including amyotrophic lateral sclerosis (ALS) and Alzheimer disease¹.

The glutamate transporter family includes five human EAAT subtypes (EAAT1 through EAAT5), two neutral amino acid transporters and several prokaryotic homologs². Glutamate transport by EAATs is coupled to the cotransport of three Na⁺ ions and one proton and the countertransport of one K⁺ ion³. In addition to this stoichiometrically coupled transport, Na⁺-dependent glutamate binding to the EAATs activates an uncoupled anion conductance, which is known to be important for EAAT physiology at some synapses⁴⁻⁸. Although this uncoupled anion conductance requires glutamate and Na⁺ binding to the transporter, it is independent of the rate or direction of glutamate transport^{7,9-13}. Though some prokaryotic family members couple transport to Na⁺, others use a proton gradient as an energy source¹⁴. Little is known about the further details of transport in these prokaryotic family members.

A recent crystal structure of a glutamate transporter homolog from *Pyrococcus horikoshii* (Glt_{ph})¹⁵ reveals the complex architecture of this transporter family and offers the possibility of new approaches to understanding the structural basis of its transport mechanism. Features of the Glt_{ph} trimer suggest that it can serve as a structural

model for understanding transport in the EAATs¹⁶: Glt_{ph} shares about 36% amino acid identity with the EAATs, and many of the EAAT residues that have been implicated in glutamate and ion binding or translocation^{13,17,18} and chloride permeation¹⁹ are highly conserved throughout the family. The structure also agrees with biochemical experiments on bacterial^{20,21} and mammalian²²⁻²⁸ transporters demonstrating the functional importance of the highly conserved C-terminal domain, which includes two reentrant loops, HP1 and HP2.

To fully understand the mechanistic implications of the Glt_{ph} structure, it is necessary to understand the transporter's basic functional properties. Only those mechanistic features that are conserved between bacterial and mammalian homologs can be understood in detail by analyzing the Glt_{ph} structure. Indeed, though both Glt_{ph} and the EAATs transport negatively charged amino acids coupled to a Na⁺ gradient, they differ in their specificity: EAATs transport glutamate and aspartate with similar affinities²⁹ whereas Glt_{ph} is an aspartate transporter with relatively low affinity for glutamate³⁰. It remains unknown whether the uncoupled chloride conductance is a conserved property of the entire family; if the bacterial transporters have this function, we could use them as tools to understand the mechanism of anion permeation. Such tools would be useful, as little is understood regarding the structural basis of EAAT anion permeation, despite its rising prominence in EAAT physiology. Indeed, there is even conflicting evidence as to the very location of the chloride permeation pathway through these transporters. Some results support a model with an individual protomer capable of both glutamate transport and chloride flux^{19,31}, whereas others suggest that chloride permeates through a pore formed at the center of the trimeric complex^{32,33}.

Membrane Transport Biophysics Unit, Porter Neuroscience Center, National Institute of Neurological Disorders and Stroke, US National Institutes of Health, 35 Convent Drive, Building 35, MSC 3701, Bethesda, Maryland 20892, USA. Correspondence should be addressed to J.A.M. (mindellj@ninds.nih.gov).

Received 12 December 2006; accepted 9 March 2007; published online 15 April 2007; doi:10.1038/nsmb1230

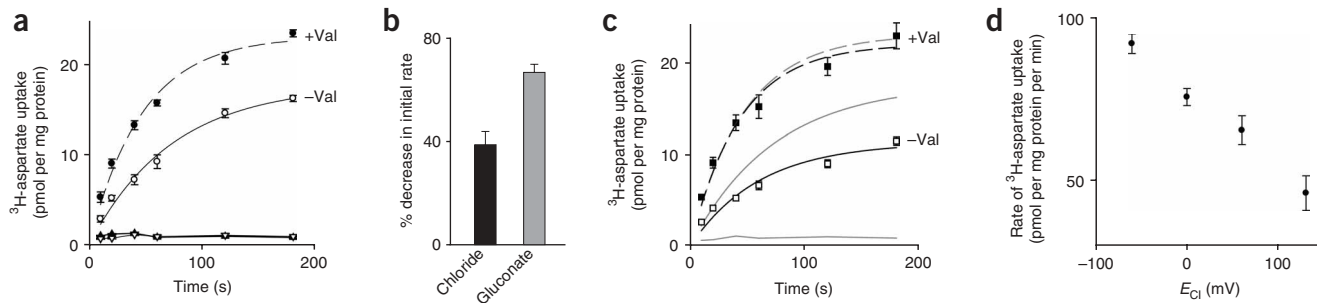


Figure 1 Glt_{Ph} has an uncoupled chloride conductance. **(a)** Valinomycin-dependent aspartate uptake by Glt_{Ph}. Glt_{Ph} proteoliposomes were added to reaction buffer in the presence of an inwardly directed Na⁺ gradient, external aspartate (10 μM L-aspartate, 75 nM ³H-L-aspartate) and a Cl⁻-containing buffer. Background levels of uptake are also shown, measured in equimolar Na⁺ (∇) or protein-free liposomes (▲). **(b)** Decrease in initial rate of uptake after removal of valinomycin, when chloride or gluconate is the anion in the reaction buffer. **(c)** Aspartate uptake in a Cl⁻-free buffer, measured as in **a** except that Glt_{Ph} proteoliposomes were added to gluconate-containing buffers in the presence or absence of valinomycin. Data from **a** is plotted in light gray for comparison. **(d)** The membrane potential of the liposome can be set by chloride. The chloride gradient across the liposome was varied, changing the driving force for chloride. Initial rate of ³H-L-aspartate uptake is plotted as a function of the equilibrium potential of chloride (E_{Cl}). Chloride concentrations (mM, in/out) were 10/100 (-58 mV), 100/100.75 (0 mV), 100/0.75 (+127 mV) or 100/10.75 (+58 mV), with the external solution defined as ground. Error bars in all graphs show s.e.m.

Given the limitations in the current understanding of the structural basis of chloride permeation and its relationship with glutamate transport, we sought to determine whether bacterial members of this family have a chloride conductance. We found that Glt_{Ph} has an uncoupled chloride conductance with similar selectivity properties to that of the EAATs. Mutating a residue analogous to one that specifically affects chloride permeation in EAAT1 has similar effects on Glt_{Ph}, suggesting that this protein can serve as a structural model for understanding anion permeation through the mammalian glutamate transporters. We also found that anion permeation is conserved in another bacterial glutamate transporter, but not in a bacterial member of the Na⁺/Cl⁻-dependent family of neurotransmitter transporters.

RESULTS

Aspartate transport by Glt_{Ph} is electrogenic

The goal of this study was to investigate whether chloride permeates Glt_{Ph} and whether this chloride movement is uncoupled to aspartate transport, as it is in the eukaryotic members of this family. We expressed Glt_{Ph} in *Escherichia coli*, purified it to homogeneity and reconstituted the pure protein into liposomes using previously described methods³⁴. In the presence of an inwardly directed Na⁺ gradient, we observed ³H-aspartate uptake into liposomes containing Glt_{Ph} (Fig. 1a). Background levels of ³H-aspartate uptake in protein-free liposomes were similar to those in the absence of a Na⁺ gradient (Fig. 1a). The low uptake under the latter condition rules out the possibility that this radioactivity represents binding to the protein without transport.

At least two Na⁺ ions are coupled to aspartate binding³⁰ and transport by Glt_{Ph} (R.M.R. and J.A.M., unpublished data). If these are the only coupled ions, a single transport cycle would result in a net inward movement of one positive charge, rendering Glt_{Ph} electrogenic. Consequently, initial cycles of aspartate transport would generate an electrical potential across the membrane, inhibiting further transport; aspartate uptake in our system should thus depend on the presence of the K⁺ ionophore valinomycin, which can dissipate the potential. Indeed, when we measured uptake in the absence of valinomycin, we observed a decrease in the initial rate of transport (~40%; Fig. 1a,b), demonstrating that transport by Glt_{Ph} is electrogenic and suggesting

that at least two Na⁺ ions are coupled to the transport of each aspartate molecule by Glt_{Ph}.

Glt_{Ph} has an uncoupled chloride conductance

Notably, we observed a substantial amount of uptake even in the absence of valinomycin. Upon first consideration, one might expect the residual level of aspartate transport in the absence of valinomycin to be vanishingly small, as chemically insignificant amounts of charge movement can generate large transmembrane voltages. A rough calculation (see **Supplementary Discussion** online) suggests that ~7 nmol of aspartate would have to move per mg of lipid to generate a membrane potential that would inhibit transport. We observed ~75 nmol of total aspartate movement per mg lipid, suggesting that there is another component in this system that can substitute for valinomycin and dissipate the transport-generated voltage. By analogy with the eukaryotic glutamate transporters, a likely candidate for this role would be a chloride conductance in the transporter itself. We hypothesized that Glt_{Ph} is also permeable to Cl⁻ and that movement of Cl⁻ is responsible for partially dissipating the electrical potential across the membrane in the absence of valinomycin. This hypothesis predicts that removing chloride from our reaction buffer should reduce transport in the absence of valinomycin.

To investigate this possibility, we substituted chloride in our external solutions with gluconate, an anion which is impermeant to the EAATs^{7,10,12}. Indeed, levels of uptake in a gluconate buffer are markedly lower than in a Cl⁻ buffer in the absence of valinomycin (Fig. 1c). Though the initial rates in the presence of valinomycin are indistinguishable, removal of valinomycin decreases the initial rate of uptake by ~70% when gluconate is the external anion compared with ~40% when chloride is the external anion (Fig. 1b). This stronger valinomycin dependence in the absence of Cl⁻ supports the assertion that aspartate transport by Glt_{Ph} is electrogenic and demonstrates that Cl⁻ can partially dissipate the transport-generated transmembrane voltage. As we observed aspartate transport in the absence of Cl⁻, these experiments also demonstrate that Cl⁻ is not stoichiometrically coupled to aspartate transport. Thus, like the EAATs, Glt_{Ph} can mediate uncoupled chloride movement across the membrane.

If, as we suggest, Cl⁻ is permeant through Glt_{Ph}, we should be able to set the membrane potential of the liposome simply by changing the

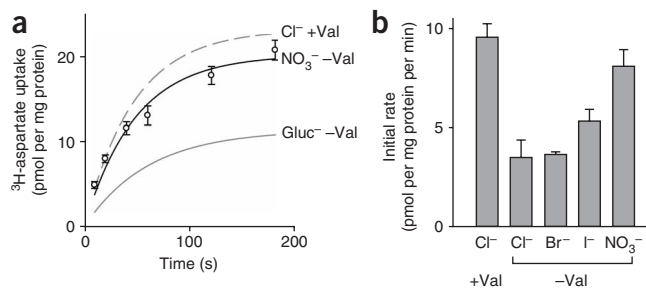


Figure 2 Anion dependence of aspartate transport. **(a)** Aspartate transport in NO_3^- buffer in the absence of valinomycin (-Val). For reference, data from **Figure 1a,c** are also shown. **(b)** Initial rate of uptake (measured as in **Fig. 2a**) in solutions containing various monovalent anions, in the absence of valinomycin. For reference, results in the presence of valinomycin are shown for Cl^- buffer. Rates were corrected by subtracting the initial rate of uptake in gluconate -Val, which was taken as baseline. Error bars in both graphs show s.e.m.

driving force for Cl^- ; this in turn should affect the rate of aspartate uptake. We set the liposome membrane potential by varying the internal and external Cl^- concentration (balancing ionic strength with an impermeant anion, CH_3SO_3^-) and measured ^3H -aspartate uptake in the absence of valinomycin (**Fig. 1d**). When the chloride driving force is set so that there is an inside negative potential ($E_{\text{Cl}} = -58$ mV) the initial rate of uptake is greater than when Cl^- is equal on both sides ($E_{\text{Cl}} = 0$ mV). Furthermore, when $E_{\text{Cl}} = +58$ mV, transport is reduced, and a more positive potential of $+127$ mV further reduces transport. These results demonstrate that Cl^- is sufficiently permeable through Glt_{ph} to set the membrane potential of the liposome and reinforce the finding that transport by Glt_{ph} is electrogenic with a net inward transfer of positive charge. The observation of different rates of uptake at -58 and 0 mV also reveals that the effect of Cl^- is not an allosteric modulation of transport activity by external Cl^- , as the only change between these measurements is the internal chloride concentration.

Glt_{ph} anion selectivity sequence

In a Cl^- -containing buffer, the addition of valinomycin still results in an increase in transport, indicating that Cl^- can only partially compensate for valinomycin in dissipating the membrane potential. If the anion movement through the transporter is rate limiting for aspartate transport, our hypothesis predicts that replacing Cl^- with a more permeant anion will further increase the initial rate of transport in the absence of valinomycin. The uncoupled chloride conductance of the EAATs has the following selectivity sequence: gluconate \lll $\text{Cl}^- < \text{Br}^- < \text{I}^- < \text{NO}_3^- < \text{SCN}^-$, where SCN^- is the most permeant anion and gluconate is impermeant^{7,10,12}. When we replaced Cl^- in the reaction buffer with NO_3^- , the initial rate of aspartate uptake was higher than in both gluconate and Cl^- , actually approaching the level of uptake in the presence of valinomycin (**Fig. 2a**). This suggests that NO_3^- is nearly as good as valinomycin at dissipating the transport-generated potential.

The abilities of different anions to increase transport in the absence of valinomycin can be used as a rough measure of the relative permeabilities of these anions through the Glt_{ph} anion pathway. Taking the initial rate of uptake in gluconate as background, we subtracted it and plotted the initial rates of uptake in various external anions (in the absence of valinomycin; **Fig. 2b**). We did not test SCN^- in these experiments because it is known to permeate the lipid

membrane and would confound our results³⁵. The order of the anions' ability to support uptake ($\text{Cl}^- \approx \text{Br}^- < \text{I}^- < \text{NO}_3^-$) is very similar to the selectivity sequence of the uncoupled anion conductance of the EAATs ($\text{Cl}^- < \text{Br}^- < \text{I}^- < \text{NO}_3^-$), hinting that uncoupled chloride movement is conserved between evolutionarily distant members of the glutamate transporter family.

Direct measurement of chloride movement

All of the previous experiments rely on monitoring effects on aspartate transport to report chloride permeation through Glt_{ph} . We directly assessed movement of chloride through the transporter by using the fluorescent indicator 6-methoxy-*N*-(3-sulfopropyl)quinolinium, inner salt (SPQ), which is quenched by Cl^- but not by NO_3^- (ref. 36). Glt_{ph} liposomes loaded with SPQ and a NaNO_3 buffer were added to Cl^- -containing buffers, and changes in fluorescence were monitored. Under these conditions, NO_3^- and Cl^- , which both permeate Glt_{ph} , should exchange electroneutrally through the transporter. If Cl^- accumulates in the liposomes, it will increasingly quench the enclosed SPQ.

We observed a large initial increase in fluorescence upon addition of either Glt_{ph} or protein-free liposomes owing to the unquenched SPQ contained within the liposomes; we normalized the data in each trace to a value measured immediately after the mixing artifact, typically < 10 s after addition (**Fig. 3a**, representative traces). The fluorescence of Glt_{ph} liposomes in the presence of Na^+ and 1 mM aspartate decreased dramatically, without leveling off for the remainder of the experiment, ultimately reaching a value of $70\% \pm 3\%$ (**Fig. 3a**, red trace, $n = 3$) of its initial value. In contrast, the fluorescence of protein-free liposomes relaxed minimally, to a level of $98\% \pm 2\%$ (**Fig. 3a**, black trace, $n = 5$). The large decrease in fluorescence in the Glt_{ph} -containing liposomes is due to the quenching of SPQ by chloride and directly reveals the movement of both Cl^- and NO_3^- through Glt_{ph} .

We investigated the behavior of this anion flux by manipulating the composition of the external solution. Removing aspartate from the buffer resulted in a substantially decreased rate of chloride influx (**Fig. 3a**, green trace). Substituting Na^+ with K^+ in the external buffer

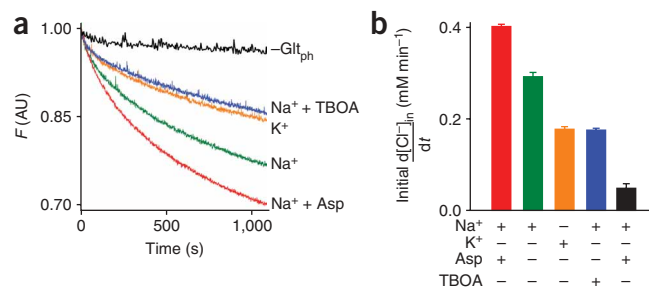


Figure 3 Direct measurement of Glt_{ph} anion permeation. **(a)** Glt_{ph} (colored lines) or protein-free (black line) liposomes loaded with 100 mM NaNO_3 and SPQ were introduced at time 0 into a buffer containing 100 mM NaCl plus 1 mM L-aspartate (red trace), 100 mM NaCl (green trace), 100 mM KCl (orange trace) or 100 mM NaCl and 1 mM TBOA (blue trace). For each, a representative fluorescence emission trace at 430 nm (excitation at 350 nm) is plotted over the 18-min duration of an experiment. Data were normalized to the initial fluorescence value. AU, arbitrary units. **(b)** Initial rates of change in $[\text{Cl}^-]_{\text{in}}$ calculated from the data in **a** and the Stern-Volmer equation, with $K_{\text{sv}} = 118$ M^{-1} (ref. 36). The bar graph is colored as in **a**. At the beginning of the experiment, $[\text{Cl}^-]_{\text{in}}$ is assumed to be 0 mM. Error bars show s.e.m.

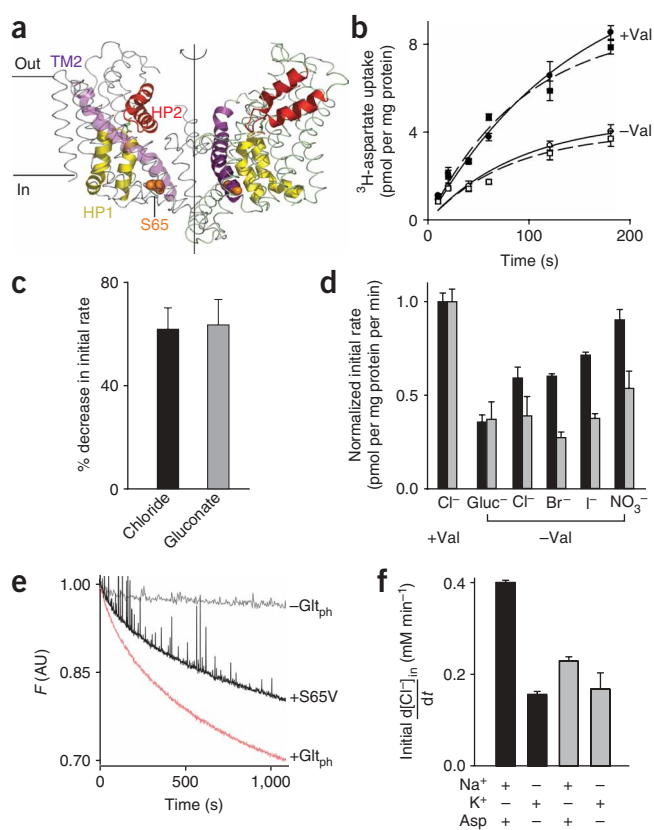


Figure 4 Glt_{Ph}S65V has altered anion permeation. **(a)** Two protomers of Glt_{Ph} shown in ribbon representation; the third protomer is removed for clarity (PDB 2NWL). HP1 (yellow), HP2 (red) and TM2 (purple) are highlighted in cartoon representation, Ser65 (orange) is shown in space-filling representation and bound aspartate is shown in stick representation. Black line represents three-fold symmetry axis. Structures were viewed and rendered in PyMOL (<http://www.pymol.org>)⁵⁰. **(b)** The S65V mutation was introduced into Glt_{Ph} and aspartate uptake was measured as in **Figure 1a**, in either Cl⁻ (circles) or gluconate (squares) buffer, in the presence or absence of valinomycin (Val). **(c)** Decrease in the initial rate of uptake in **b** after removal of valinomycin, when chloride or gluconate is the anion in the reaction buffer. **(d)** Initial rates of uptake for wild-type (black) or S65V (gray) in buffers containing different monovalent anions in the absence of valinomycin. Data were normalized to the initial rate of uptake in Cl⁻ buffer in the presence of valinomycin (shown for reference). **(e)** Fluorescence Cl⁻/NO₃⁻ experiments as in **Figure 3a**, comparing chloride flux from wild-type and S65V Glt_{Ph}. Liposomes loaded with 100 mM NaNO₃ and SPQ were diluted into an external buffer containing 100 mM NaCl and 1 mM L-aspartate. Protein-free and Glt_{Ph} data are reproduced from **Figure 3a** for comparison. **(f)** Initial rates of change in [Cl⁻]_{in}, calculated as in **Figure 3b**, for wild-type Glt_{Ph} (black) and Glt_{Ph}-S65V (gray). Error bars in all graphs show s.e.m.

S65V mutation

Our results demonstrating that Glt_{Ph} has an uncoupled chloride conductance with striking similarities to that of its mammalian cousins raise the possibility that this structurally characterized protein can serve as a model to understand the mechanism of chloride permeation in the EAATs. We examined the Cl⁻ transport mechanism by making a mutation in Glt_{Ph} analogous to one in EAAT1 (S103V) that strongly affects the chloride conductance without measurable effects on glutamate transport¹⁹. This residue aligns with Ser65 in Glt_{Ph}, located in transmembrane domain-2 (TM2) (**Fig. 4a**); we mutated it to valine and examined the transport properties of Glt_{Ph}-S65V.

In Glt_{Ph}, this mutation had little effect on Na⁺-dependent aspartate transport but profoundly affected chloride conductance. The S65V transporter shows comparable levels of aspartate uptake in Cl⁻ or gluconate buffer in the absence of valinomycin (**Fig. 4b**), a strong contrast to wild-type transporter (**Fig. 1a,c**). A similar reduction of uptake under either condition upon the removal of valinomycin (**Fig. 4c**) demonstrates that the cycle remains electrogenic but that there is insufficient uncoupled anion movement remaining to dissipate the transport-generated potential. Furthermore, replacing Cl⁻ with alternative monovalent anions has little effect on uptake, another marked departure from the wild-type behavior (**Fig. 4d**).

We verified the effects of the mutation using the SPQ assay to measure chloride flux directly. We observed considerably reduced chloride flux for the S65V mutant: in the presence of Na⁺ and 1 mM aspartate, the initial rate of chloride movement into the S65V liposomes is ~40% less than that for Glt_{Ph} liposomes (**Fig. 4e,f**). Furthermore, the ability of Na⁺ and aspartate to activate Cl⁻ flux (as compared with the level of Cl⁻ movement observed when K⁺ is the external cation) is impaired by the S65V mutation (**Fig. 4f**). These results strongly suggest that anions permeate through a specific pathway in the transporter that can be disrupted without affecting aspartate transport, and that this pathway is similar to the chloride permeation pathway of the EAATs. Thus, Glt_{Ph} can serve as a tool for understanding the structural mechanisms of anion permeation in the mammalian EAATs.

Uncoupled chloride conductance is not unique to Glt_{Ph}

To determine whether other bacterial transporters might also have chloride conductances, we repeated similar chloride-dependence

further reduced the chloride flux but did not abolish it entirely (**Fig. 3a**, orange trace). Similarly, addition of the transport inhibitor D,L-threo-β-benzoyloxyspartate (TBOA)³⁰ reduced the chloride flux, but not to background levels (**Fig. 3a**, blue trace). The activation of chloride movement by Na⁺ and aspartate corresponds well with observed behaviors of the EAATs, which show both glutamate-activated and Na⁺-activated (termed 'leak') chloride conductances. In contrast, residual chloride currents have not been described previously for the EAATs in the absence of Na⁺ or in the presence of TBOA. However, EAAT anion currents are usually defined by TBOA block (which requires the presence of Na⁺), and the measurements are made in systems with other baseline conductances (for example, *Xenopus laevis* oocytes). It is therefore difficult to determine whether the chloride fluxes we observed in the absence of Na⁺ or in the presence of TBOA exist in the EAATs (but have not been observed because of these experimental limitations) or whether they represent a unique property of the bacterial transporter. Experiments using purified EAATs reconstituted in liposomes may be required to resolve this question.

Assuming that the Cl⁻ concentration inside the liposomes is zero ([Cl⁻]_{in} = 0) at the moment we start the fluorescence experiment, we can use the Stern-Volmer equation to convert the change in fluorescence of SPQ to a change in [Cl⁻]_{in} and estimate the initial rates of chloride flux under each condition (**Fig. 3b**). In the presence of Na⁺ and aspartate, this rate is 0.4 mM min⁻¹. Assuming that our vesicles are uniform with a radius of 50 nm³⁷, we calculate a rate of chloride flux of roughly 44 nmol per mg protein per min, ~22-fold higher than the initial rate of aspartate transport (2 nmol per mg protein per min) by Glt_{Ph} (calculated from uptake measurements; see **Supplementary Discussion**). The large difference between the rates of aspartate and Cl⁻ uptake provides further support for an uncoupled mechanism of anion permeation.

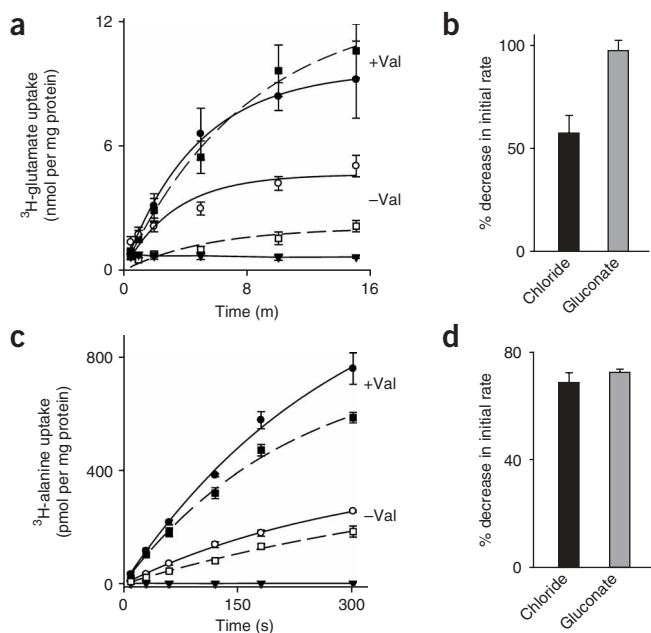


Figure 5 Chloride dependence of uptake in other bacterial transporters. (a) Proton-driven ^3H -glutamate uptake was measured for GltT_{BS} in Cl^- (circles) or gluconate (squares) buffer in the presence or absence of valinomycin (Val). Triangles show background uptake in the absence of a proton gradient. (b) Decrease in initial rate of uptake in a after removal of valinomycin, when chloride or gluconate is the anion in the reaction buffer. (c) Na^+ -driven uptake of ^3H -alanine was measured for LeuT_{AA} , as in a. Triangles show background uptake in the absence of an Na^+ gradient. (d) Decrease in the initial rate of uptake in c after removal of valinomycin, as in b. Error bars in all graphs show s.e.m.

experiments on two other proteins. The first, GltT_{BS} , is another member of the glutamate transporter family, cloned from the thermophile *Bacillus stearothermophilus*; it shares $\sim 27\%$ amino acid identity with the EAATs and $\sim 37\%$ amino acid identity with GltP_{H} . Although GltT_{BS} is part of the same gene family, it is quite different from both GltP_{H} and the EAATs, as it is a proton-driven transporter that can effectively transport both glutamate and aspartate¹⁴.

We expressed, purified and reconstituted GltT_{BS} protein into liposomes and studied the effect of valinomycin on transport rates in the presence of Cl^- or gluconate. Glutamate uptake by GltT_{BS} is stimulated by valinomycin (Fig. 5a), in agreement with a previous study in membrane vesicles of *B. stearothermophilus*¹⁴. As with GltP_{H} , replacing chloride with gluconate further decreases transport by GltT_{BS} in the absence of valinomycin (Fig. 5a), and the decrease in uptake upon removal of valinomycin is substantially larger when the outside buffer contains gluconate than when it contains chloride (Fig. 5b). These results indicate that GltT_{BS} also mediates uncoupled chloride movement and suggest that this phenomenon is a general characteristic of the glutamate transporter family.

The third transporter we investigated is LeuT_{AA} , a member of the Na^+/Cl^- -dependent family of neurotransmitter transporters from *Aquifex aeolicus*³⁸. LeuT_{AA} is a Na^+ -dependent alanine transporter (S. Singh and E. Gouaux, Vollum Institute, personal communication) that shares $\sim 19\%$ amino acid identity with eukaryotic members of this family, which include transporters for dopamine, serotonin, γ -amino butyric acid (GABA) and noradrenaline³⁸. Several mammalian transporters in this family also conduct ions, in a process that is thermodynamically uncoupled from the transport of substrate^{39–44}.

In the case of the dopamine transporter (DAT), substrate-activated chloride conductance has been observed in cells of both *Caenorhabditis elegans*⁴⁵ and rat, and in rat it has been shown to have a physiological function in regulating presynaptic excitability⁴¹.

In agreement with a previous study³⁸, we also observed that transport by LeuT_{AA} is electrogenic and requires only a Na^+ gradient (Fig. 5c). Transport is not coupled to Cl^- , which makes this bacterial homolog different from the mammalian transporters in its family but similar to a bacterial tyrosine transporter from *Fusobacterium nucleatum* (Tyt1)⁴⁶. In our assay, removal of chloride from the reaction buffer in the absence of valinomycin has no effect on transport (Fig. 5c,d), suggesting that LeuT_{AA} does not have an uncoupled chloride conductance or that the selectivity of this pathway differs from the eukaryotic members of the Na^+/Cl^- -dependent family.

DISCUSSION

While investigating the transport mechanism of GltP_{H} , we noted that despite clear evidence of its electrogenicity, substantial transport occurs in the absence of valinomycin. Exploration of this phenomenon revealed that, like its mammalian cousins, GltP_{H} catalyzes transmembrane chloride movement thermodynamically uncoupled from Na^+ -dependent aspartate transport. We also found that, in the absence of valinomycin, several different anions can support transport, in the order $\text{Cl}^- \approx \text{Br}^- < \text{I}^- < \text{NO}_3^-$, a selectivity sequence very similar to that of the EAATs. In the absence of any other pathway to allow the dissipation of the transporter-generated voltage, GltP_{H} can act like a chloride ionophore and, by allowing anions to passively diffuse down their gradients, can set the membrane potential of the liposome and thus influence the rate of aspartate transport. In addition, using a fluorescence-based assay, we directly demonstrated chloride flux through GltP_{H} in the form of $\text{Cl}^-/\text{NO}_3^-$ exchange. Like that of the EAATs, this flux is stimulated by both Na^+ and substrate and is inhibited by TBOA.

These results not only demonstrate a specific, GltP_{H} -mediated path for chloride through the membrane but also hint at a physiological role for the uncoupled chloride conductance. In agreement with the physiological role proposed for such a conductance in a retinal glutamate transporter⁴, the uncoupled chloride conductance of GltP_{H} is able to hyperpolarize the membrane and may represent a built-in mechanism common to all members of the glutamate transporter family, used to dissipate the electrical potential generated during substrate transport.

In GltP_{H} , the S65V mutation results in a functional aspartate transporter that lacks the ability to utilize anions to drive transport in the absence of valinomycin and shows reduced Cl^- flux in a direct assay. These results further support the notion that chloride interacts directly with GltP_{H} and also suggest that the chloride permeation pathways of GltP_{H} and EAAT1 are similar. Further evidence of this broad conservation comes from the observation that a proton-dependent glutamate transporter, GltT_{BS} , also shows uncoupled chloride flux. In the face of considerable divergence in both sequence and function, these results suggest strong evolutionary pressure to maintain the chloride pathway. Insofar as the mechanism of chloride permeation is conserved between the bacterial transporters and the EAATs, GltP_{H} will prove invaluable as a structural model for probing the molecular interactions underlying anion flux in all members of the glutamate transporter family.

Such a structural model will be particularly useful given the current disagreements over many facets of EAAT anion conduction. Although there is general agreement that individual monomers in the trimeric complex transport glutamate independently^{31,47} and the structure of GltP_{H} shows three aspartate binding sites, each one entirely contained

within a single protomer^{15,30}, there is still disagreement over the chloride pathway. Does chloride permeate a central pore formed along the symmetry axis of the trimer, similarly to a ligand-gated ion channel³², or does each individual monomer allow chloride permeation, as is observed in the ClC chloride transporter⁴⁸? Now that we have established definitively that Glt_{ph} has an uncoupled chloride conductance with similar properties to that of the EAATs, we can make inferences by examining functional data from EAATs together with structural and functional data from Glt_{ph}.

There is no apparent aqueous pathway at the interface of the three subunits in the Glt_{ph} structure—indeed, the residues in this region are particularly hydrophobic. Thus, it seems unlikely that the trimer interface would act as a pore allowing anion diffusion through the membrane. In addition, the residue in TM2 that affects chloride permeation properties in both EAAT1 and Glt_{ph} is not at the trimer interface but rather lies on a solvent-accessible face of TM2 that faces toward the substrate-binding domain (see Fig. 4a). We propose that the Glt_{ph} chloride pathway proceeds along TM2 and is very similar to the chloride pathway in the EAATs¹⁹. If our model is accurate, then conformational changes underlying substrate transport could easily be involved in regulating chloride permeation. Recent results show a movement of the HP2 hairpin upon binding of substrate and Na⁺ to the transporter; similar movements have been proposed for HP1 (ref. 30). Given that the side of TM2 that includes Ser65 faces these hairpins (see Fig. 4a), it is easy to imagine that movements of HP1 and HP2 could affect chloride conduction as well as substrate transport. Further functional and structural experiments will be required to test this hypothesis.

Although the uncoupled chloride conductance is apparently ubiquitous in the glutamate transporter family, we have established that it is not a general feature of all bacterial transporters. Many reports have documented that a variety of mammalian neurotransmitter transporters belonging to the Na⁺/Cl⁻-dependent transporter family carry uncoupled conductances, but in this case, the conductances do not seem to be evolutionarily essential, as we have observed for LeuT_{Aa}. In retrospect, this is perhaps not surprising, as the ions that carry the uncoupled conductances are quite varied in this family and at least one member (the glycine transporter) has not been found to have any uncoupled conductances⁴⁹.

This work is the first demonstration of an uncoupled anion conductance in any bacterial transporter; it reveals that the chloride conductance of the glutamate transporters is conserved through evolution and may be an essential feature of the transport mechanism in this family. We can now use the structure of Glt_{ph} to aid in probing the mechanism of chloride permeation through the EAATs, to better understand the physiological role of this conductance and its structural basis in a protein that can act as both a transporter and a channel.

METHODS

Mutagenesis and biochemistry. The S65V mutation was introduced into Glt_{ph} using the QuikChange mutagenesis kit (Stratagene). The presence of the introduced mutation, and absence of any other changes, was confirmed by sequencing both strands of the entire coding region of the gene (National Institute of Neurological Disorders and Stroke DNA sequencing facility). Glt_{ph}, Glt_{ph}-S65V, Glt_{Bs} and LeuT_{Aa} proteins were purified essentially as described^{15,34,38}, with the following modifications. Membranes were isolated and solubilized with *n*-dodecyl-β-D-maltopyranoside (Anatrace) and protein was initially purified using nickel-nitrilotriacetic acid resin (GE Healthcare). The histidine tag was subsequently removed by digestion with thrombin (10 U mg⁻¹) and the protein further purified on a size-exclusion column where the detergent was exchanged to *n*-decyl-β-D-maltopyranoside (Anatrace).

Pure protein was reconstituted into liposomes as described³⁴. Briefly, *Escherichia coli* polar lipids and 1-palmitoyl-2-oleoyl-*sn*-glycero-3-phosphocholine (Avanti Polar Lipids) at a ratio of 3:1 were mixed, dried under nitrogen and resuspended in 100 mM potassium phosphate (pH 7.4) or the appropriate inside solution, as indicated in the figure legends. Liposomes were formed by extrusion through 400-nm membranes (Avanti Polar Lipids) and were treated with either 0.5% or 2.5% (w/w) Triton X-100 (Anatrace) before protein was added at 3–50 μg protein per mg lipid. The protein-lipid mixture was left at room temperature for 30 min, after which biobeads (Bio-Rad) that had been extensively prewashed with methanol and water and equilibrated in resuspension buffer were added (80 mg ml⁻¹) to the protein-lipid mixture to remove detergent. After 2 h incubation at room temperature with gentle agitation, the biobeads were removed by filtration and fresh biobeads were added. After a further 2 h incubation at 4 °C, another batch of biobeads was added and the protein-lipid mixture was further incubated at 4 °C overnight. Proteoliposomes were concentrated, resuspended at 100 mg lipid ml⁻¹ (0.3–5.0 mg protein per ml) and either used immediately or flash-frozen in a bath of dry ice and ethanol and stored at –80 °C.

Transport assay. For Glt_{ph}, proteoliposomes were loaded with 100 mM KCH₃SO₃ and 20 mM HEPES (pH 7.5) and the uptake reaction was initiated by diluting them (100 mg lipid ml⁻¹) 133-fold into reaction buffer prewarmed to 30 °C. The reaction buffer contained 100 mM NaX (X = gluconate, Cl⁻, Br⁻, I⁻ or NO₃⁻), 20 mM HEPES (pH 7.5), 10 μM L-aspartate and 75 nM ³H-L-aspartate (GE Healthcare). These represent saturating concentrations of substrate (*K_m* = 100 nM; R.M.R. and J.A.M., unpublished observations). Background levels of ³H-L-aspartate uptake in protein-free liposomes or Glt_{ph} liposomes with equimolar K⁺ or Na⁺ on either side of the membrane were indistinguishable from one another.

Glt_{Bs} liposomes were loaded with 100 mM CH₃COOK and 20 mM HEPES (pH 7.5) and diluted as described above into a reaction buffer containing 100 mM NaX (X = gluconate, Cl⁻, Br⁻, I⁻ or NO₃⁻), 20 mM MES (pH 5.0) and 40 nM ³H-L-glutamate. LeuT_{Aa} experiments were identical to those with Glt_{ph}, except that 100 nM ³H-L-alanine was used and no unlabeled substrate was present (we also performed similar experiments in the presence of 10 μM unlabeled L-alanine, with the same result). Plus-valinomycin (+Val) conditions contained 1 μM valinomycin (from a 1 mM stock in ethanol). The addition of ethanol alone had no effect on aspartate transport (data not shown). At each time point, a 200-μl aliquot was removed and diluted 1,000-fold into ice-cold quenching buffer (100 mM LiCl, 20 mM HEPES (pH 7.5)), then immediately filtered over nitrocellulose filters (0.22-mm pore size, Millipore). The filters were washed once with 2 ml of ice-cold quenching buffer and assayed for radioactivity using a Trilux β counter (Perkin Elmer).

In the anion-dependence experiments, the impermeant anion CH₃SO₃⁻ was used in the inside buffer to create an equal inward driving force for all external anions. Experiments where the membrane potential was set by the chloride equilibrium potential (*E_{Cl}*) were done in the absence of valinomycin. Osmolarity was balanced with CH₃SO₃⁻ and the reaction buffer contained 100 nM ³H-aspartate. All initial rates were calculated from the linear portion of the curve (first 30 s) and all data represent the mean and s.e.m. of at least three experiments. Uptake data are fit to single exponentials for presentation.

Chloride-based fluorescence assay. Glt_{ph}, Glt_{ph}-S65V or protein-free liposomes were loaded with inside buffer (100 mM NaNO₃, 20 mM HEPES (pH 7.5), 300 μM SPQ (Molecular Probes)) and extruded through 400-nm membranes. Immediately before each experiment, 100 μl of liposomes (5 mg lipid per ml) were spun through a 5-ml Sephadex column pre-equilibrated in the same buffer without SPQ, and liposomes were added to 3 ml outside buffer (100 mM NaCl or KCl, 20 mM HEPES (pH 7.5), 1 mM L-aspartate or 1 mM TBOA) in a quartz cuvette. Fluorescence changes were detected with a Fluoromax-3 (Jobin Yvon) fluorescence spectrophotometer, equipped with Peltier temperature control (*T* = 22 °C). Excitation wavelength was 350 nm and emission wavelength was 430 nm.

Note: Supplementary information is available on the Nature Structural & Molecular Biology website.

ACKNOWLEDGMENTS

We thank E. Gouaux (Vollum Institute and Howard Hughes Medical Institute, Oregon Health and Science University) for providing GlT_{Ph} and LeuT_{Aa} plasmids, J. Lolkema (University of Groningen) for providing GlT_{Bs} plasmid, S. Singh and E. Gouaux for sharing unpublished results, K. Swartz for incisive comments on the manuscript and P. Curran for expert technical support. R.M.R. is funded by an Australian National Health and Medical Research Council C.J. Martin Postdoctoral Fellowship (ID358779). This work was supported by the US National Institute of Neurological Disorders and Stroke intramural program.

COMPETING INTERESTS STATEMENT

The authors declare they have no competing financial interests.

Published online at <http://www.nature.com/nsmb>

Reprints and permissions information is available online at <http://npg.nature.com/reprintsandpermissions>

- Danbolt, N.C. Glutamate uptake. *Prog. Neurobiol.* **65**, 1–105 (2001).
- Slotboom, D.J., Konings, W.N. & Lolkema, J.S. Structural features of the glutamate transporter family. *Microbiol. Mol. Biol. Rev.* **63**, 293–307 (1999).
- Zerangue, N. & Kavanaugh, M.P. Flux coupling in a neuronal glutamate transporter. *Nature* **383**, 634–637 (1996).
- Veruki, M.L., Morkve, S.H. & Hartveit, E. Activation of a presynaptic glutamate transporter regulates synaptic transmission through electrical signaling. *Nat. Neurosci.* **9**, 1388–1396 (2006).
- Grant, G.B. & Dowling, J.E. On bipolar cell responses in the teleost retina are generated by two distinct mechanisms. *J. Neurophysiol.* **76**, 3842–3849 (1996).
- Otis, T.S., Kavanaugh, M.P. & Jahr, C.E. Postsynaptic glutamate transport at the climbing fiber-Purkinje cell synapse. *Science* **277**, 1515–1518 (1997).
- Billups, B., Rossi, D. & Attwell, D. Anion conductance behavior of the glutamate uptake carrier in salamander retinal glial cells. *J. Neurosci.* **16**, 6722–6731 (1996).
- Eliasof, S. & Jahr, C.E. Retinal glial cell glutamate transporter is coupled to an anionic conductance. *Proc. Natl. Acad. Sci. USA* **93**, 4153–4158 (1996).
- Fairman, W.A., Vandenberg, R.J., Arriza, J.L., Kavanaugh, M.P. & Amara, S.G. An excitatory amino-acid transporter with properties of a ligand-gated chloride channel. *Nature* **375**, 599–603 (1995).
- Wadiche, J.L., Amara, S.G. & Kavanaugh, M.P. Ion fluxes associated with excitatory amino acid transport. *Neuron* **15**, 721–728 (1995).
- Wadiche, J.L., Arriza, J.L., Amara, S.G. & Kavanaugh, M.P. Kinetics of a human glutamate transporter. *Neuron* **14**, 1019–1027 (1995).
- Wadiche, J.L. & Kavanaugh, M.P. Macroscopic and microscopic properties of a cloned glutamate transporter/chloride channel. *J. Neurosci.* **18**, 7650–7661 (1998).
- Vandenberg, R.J., Arriza, J.L., Amara, S.G. & Kavanaugh, M.P. Constitutive ion fluxes and substrate binding domains of human glutamate transporters. *J. Biol. Chem.* **270**, 17668–17671 (1995).
- Tolner, B., Ubbink-kok, T., Poolman, B. & Konings, W.N. Cation-selectivity of the L-glutamate transporters of *E. coli*, *B. stearothermophilus* and *B. caldotenax*: dependence on the environment in which the proteins are expressed. *Mol. Microbiol.* **18**, 123–133 (1995a).
- Yernool, D., Boudker, O., Jin, Y. & Gouaux, E. Structure of a glutamate transporter homologue from *Pyrococcus horikoshii*. *Nature* **431**, 811–818 (2004).
- Yernool, D., Boudker, O., Folta-Stogniew, E. & Gouaux, E. Trimeric subunit stoichiometry of the glutamate transporters from *Bacillus caldotenax* and *Bacillus stearothermophilus*. *Biochemistry* **42**, 12981–12988 (2003).
- Bendahan, A., Armon, A., Madani, N., Kavanaugh, M.P. & Kanner, B.I. Arginine 447 plays a pivotal role in substrate interactions in a neuronal glutamate transporter. *J. Biol. Chem.* **275**, 37436–37442 (2000).
- Kavanaugh, M.P., Bendahan, A., Zerangue, N., Zhang, Y. & Kanner, B.I. Mutation of an amino acid residue influencing potassium coupling in the glutamate transporter GLT-1 induces obligate exchange. *J. Biol. Chem.* **272**, 1703–1708 (1997).
- Ryan, R.M., Mitrovic, A.D. & Vandenberg, R.J. The chloride permeation pathway of a glutamate transporter and its proximity to the glutamate translocation pathway. *J. Biol. Chem.* **279**, 20742–20751 (2004).
- Slotboom, D.J., Konings, W.N. & Lolkema, J.S. Cysteine-scanning mutagenesis reveals a highly amphipathic, pore-lining membrane-spanning helix in the glutamate transporter GlT. *J. Biol. Chem.* **276**, 10775–10781 (2001).
- Slotboom, D.J., Sobczak, I., Konings, W.N. & Lolkema, J.S. A conserved serine-rich stretch in the glutamate transporter family forms a substrate-sensitive reentrant loop. *Proc. Natl. Acad. Sci. USA* **96**, 14282–14287 (1999).
- Grunewald, M., Bendahan, A. & Kanner, B.I. Biotinylation of single cysteine mutants of the glutamate transporter GLT-1 from rat brain reveals its unusual topology. *Neuron* **21**, 623–632 (1998).
- Grunewald, M. & Kanner, B.I. The accessibility of a novel reentrant loop of the glutamate transporter GLT-1 is restricted by its substrate. *J. Biol. Chem.* **275**, 9684–9689 (2000).
- Seal, R.P. & Amara, S.G. A reentrant loop domain in the glutamate carrier EAAT1 participates in substrate binding and translocation. *Neuron* **21**, 1487–1498 (1998).
- Grunewald, M., Menaker, D. & Kanner, B.I. Cysteine-scanning mutagenesis reveals a conformationally sensitive reentrant pore-loop in the glutamate transporter GLT-1. *J. Biol. Chem.* **277**, 26074–26080 (2002).
- Borre, L., Kavanaugh, M.P. & Kanner, B.I. Dynamic equilibrium between coupled and uncoupled modes of a neuronal glutamate transporter. *J. Biol. Chem.* **277**, 13501–13507 (2002).
- Leighton, B.H., Seal, R.P., Shimamoto, K. & Amara, S.G. A hydrophobic domain in glutamate transporters forms an extracellular helix associated with the permeation pathway for substrates. *J. Biol. Chem.* **277**, 29847–29855 (2002).
- Ryan, R.M. & Vandenberg, R.J. Distinct conformational states mediate the transport and anion channel properties of the glutamate transporter EAAT-1. *J. Biol. Chem.* **277**, 13494–13500 (2002).
- Arriza, J.L. *et al.* Functional comparisons of three glutamate transporter subtypes cloned from human motor cortex. *J. Neurosci.* **14**, 5559–5569 (1994).
- Boudker, O., Ryan, R.M., Yernool, D., Shimamoto, K. & Gouaux, E. Coupling substrate and ion binding to extracellular gate of a sodium-dependent aspartate transporter. *Nature* **445**, 387–393 (2007).
- Grewer, C. *et al.* Individual subunits of the glutamate transporter EAAC1 homotrimer function independently of each other. *Biochemistry* **44**, 11913–11923 (2005).
- Eskandari, S., Kreman, M., Kavanaugh, M.P., Wright, E.M. & Zampighi, G.A. Pentameric assembly of a neuronal glutamate transporter. *Proc. Natl. Acad. Sci. USA* **97**, 8641–8646 (2000).
- Torres-Salazar, D. & Fahlke, C. Intersubunit interactions in EAAT4 glutamate transporters. *J. Neurosci.* **26**, 7513–7522 (2006).
- Gaillard, I., Slotboom, D., Knol, J., Lolkema, J.S. & Konings, W.N. Purification and reconstitution of the glutamate carrier GlT of the thermophilic bacterium *Bacillus stearothermophilus*. *Biochemistry* **35**, 6150–6156 (1996).
- Nicholls, D.G. *Bioenergetics: An Introduction to the Chemiosmotic Theory* (Academic Press, London; New York, 1982).
- Verkman, A.S. Development and biological applications of chloride-sensitive fluorescent indicators. *Am. J. Physiol.* **259**, C375–C388 (1990).
- Walden, M. *et al.* Uncoupling and turnover in a Cl⁻/H⁺ exchange transporter. *J. Gen. Physiol.* **129**, 317–329 (2007).
- Yamashita, A., Singh, S.K., Kawate, T., Jin, Y. & Gouaux, E. Crystal structure of a bacterial homologue of Na⁺/Cl⁻-dependent neurotransmitter transporters. *Nature* **437**, 215–223 (2005).
- Galli, A., Blakely, R.D. & DeFelice, L.J. Norepinephrine transporters have channel modes of conduction. *Proc. Natl. Acad. Sci. USA* **93**, 8671–8676 (1996).
- Galli, A., Petersen, C.I., deBlaquiere, M., Blakely, R.D. & DeFelice, L.J. *Drosophila* serotonin transporters have voltage-dependent uptake coupled to a serotonin-gated ion channel. *J. Neurosci.* **17**, 3401–3411 (1997).
- Ingram, S.L., Prasad, B.M. & Amara, S.G. Dopamine transporter-mediated conductances increase excitability of midbrain dopamine neurons. *Nat. Neurosci.* **5**, 971–978 (2002).
- Mager, S. *et al.* Conducting states of a mammalian serotonin transporter. *Neuron* **12**, 845–859 (1994).
- Mager, S. *et al.* Steady states, charge movements, and rates for a cloned GABA transporter expressed in *Xenopus* oocytes. *Neuron* **10**, 177–188 (1993).
- Risso, S., DeFelice, L.J. & Blakely, R.D. Sodium-dependent GABA-induced currents in GAT1-transfected HeLa cells. *J. Physiol. (Lond.)* **490**, 691–702 (1996).
- Carvelli, L., McDonald, P.W., Blakely, R.D. & DeFelice, L.J. Dopamine transporters depolarize neurons by a channel mechanism. *Proc. Natl. Acad. Sci. USA* **101**, 16046–16051 (2004).
- Quick, M. *et al.* State-dependent conformations of the translocation pathway in the tyrosine transporter Tyl1, a novel neurotransmitter:sodium symporter from *Fusobacterium nucleatum*. *J. Biol. Chem.* **281**, 26444–26454 (2006).
- Koch, H.P. & Larsson, H.P. Small-scale molecular motions accomplish glutamate uptake in human glutamate transporters. *J. Neurosci.* **25**, 1730–1736 (2005).
- Dutzler, R., Campbell, E.B., Cadene, M., Chait, B.T. & MacKinnon, R. X-ray structure of a Cl⁻ channel at 3.0 Å reveals the molecular basis of anion selectivity. *Nature* [comment] **415**, 287–294 (2002).
- Roux, M.J. & Supplisson, S. Neuronal and glial glycine transporters have different stoichiometries. *Neuron* **25**, 373–383 (2000).
- DeLano, W.L. *The PyMOL Molecular Graphics System* (DeLano Scientific, San Carlos, California, USA, 2002).